Inorg. Chem. **2009**, *48*, 2808−2817

Monomeric, Dimeric and Polymeric W/Cu/S Clusters Based on $[Et_4N][Tp^*W(\mu_3\text{-}S)_3(CuBr)_3]$ and Various Nitrogen Donor Ligands

Zhen-Hong Wei,[†] Hong-Xi Li,[†] Mei-Ling Cheng,[†] Xiao-Yan Tang,[†] Yang Chen,[†] Yong Zhang,[†] and Jian-Ping Lang*[,†,‡]

College of Chemistry, Chemical Engineering and Materials Science, Suzhou University, Suzhou 215123, People's Republic of China, and State Key Laboratory of Organometallic Chemistry, Shanghai Institute of Organic Chemistry, Chinese Academy of Sciences, Shanghai 200032, People's Republic of China

Received August 6, 2008

Assembly of a family of monomeric, dimeric, and polymeric W/Cu/S clusters from a precursor cluster $[Et_4N][Tp^*W(\mu_3\text{-}S)_3(CuBr)_3]$ (Tp^* = hydridotris(3,5-dimethylpyrazol-1-yl)borate) (**1**) and various N-donor ligands was reported. The treatment of **1** with pyridine (py) or aniline (ani) in the presence of NH_4PF_6 afforded a cationic cluster $[Tp^*W(\mu_3\text{-}S)_3Cu_3(py)_3(\mu_3\text{-}Br)](PF_6)$ (**2**) and a neutral cluster $[\{Tp^*W(\mu_3\text{-}S)_3(CuBr)_3\}(\mu_6\text{-}Br)\{Tp^*W(\mu_3\text{-}S)_3Cu_3(ani)_3\}]\cdot 4ani\cdot 0.5Et_2O$ (**3**$\cdot 4ani\cdot 0.5Et_2O$). On the other hand, the treatment of **1** with excess 4,4′-bipyridine (4,4′-bipy) or 1,2-bis(4-pyridyl)ethylene (bpee) followed by the addition of NH_4PF_6 led to the formation of a polymeric cluster $\{[Tp^*W(\mu_3\text{-}S)_3Cu_3(4,4'\text{-}bipy)_3(\mu_3\text{-}Br)](PF_6)\cdot H_2O\}_n$ (**4**) and a neutral cluster $[\{Tp^*W(\mu_3\text{-}S)_3Cu_3Br_2\}_2(bpee)]\cdot 0.5CH_2Cl_2$ (**5**$\cdot 0.5CH_2Cl_2$). Meanwhile, analogous reactions of **1** with excess 1,2-bis(4-pyridyl)ethane (bpe) or 1,3-bis(4-pyridyl)propane (bpp) in DMF under the presence of NH_4PF_6 resulted in the formation of two polymeric clusters $\{[\{Tp^*W(\mu_3\text{-}S)_3Cu_3(\mu_3\text{-}Br)\}_2(bpe)_3](PF_6)_2\cdot MeCN\}_n$ (**6**) and $\{[Tp^*W(\mu_3\text{-}S)_3Cu_3Br(\mu_3\text{-}Br)(bpp)]\cdot DMF\}_n$ (**7**). Compounds **1**−**7** were characterized by elemental analysis, IR spectra, UV−vis spectra, ^1H NMR, electrospray ionization mass spectra, and X-ray crystallography. The anion of **1** has an incomplete cubanelike $[Tp^*W(\mu_3\text{-}S)_3(CuBr)_3]$ structure, while the cation of **2** has a cubanelike $[Tp^*W(\mu_3\text{-}S)_3Cu_3(\mu_3\text{-}Br)]$ structure. Compound **3** may be viewed as having a corner-shared double cubanelike structure that consists of one $[Tp^*W(\mu_3\text{-}S)_3Cu_3(ani)_3]^{2+}$ dication and one $[Tp^*W(\mu_3\text{-}S)_3(CuBr)_3]^-$ anion linked by a μ_6-Br bridge. For **4**, each $[Tp^*W(\mu_3\text{-}S)_3Cu_3(\mu_3\text{-}Br)]$ unit works as a pyramidal three-connecting node to connect its equivalent ones via three 4,4′-bipy bridges to yield a 2D (6,3) cationic network. Compound **5** has a dimeric structure in which two incomplete cubanelike $[Tp^*W(\mu_3\text{-}S)_3Cu_3Br_2]$ cores are bridged with one bpee ligand. For **6**, each dimeric $[\{Tp^*W(\mu_3\text{-}S)_3Cu_3(\mu_3\text{-}Br)\}_2(bpe)_2]$ unit is interconnected via a pair of bpe bridges to form a 1D zigzag cationic chain. Compound **7** has a 1D spiral chain in which each $[Tp^*W(\mu_3\text{-}S)_3Cu_3Br(\mu_3\text{-}Br)]$ core is interlinked by a couple of bpp bridges. The formation of **2**−**7** from the precursor cluster **1** through various N-donor ligands offers a new way to the design and assembly of the W/Cu/S clusters with interesting molecular and supramolecular arrays.

Introduction

In the past decades, reactions of thiometallate anions ($[ME_xS_{4-x}]^{2-}$, $[Cp^*MS_3]^-$, and $[Tp^*WS_3]^-$; Cp^* = pentamethylcyclopentadienyl, Tp^* = hydridotris(3,5-dimethylpyrazol-1-yl)borate; M = Mo, W; E = O, S; x = 0−3) with Cu(I) and Ag(I) have been extensively investigated. This is because the Mo(W)/Cu/S clusters possess interesting structural chemistry[1−5] and potential applications in biological systems[6] and optoelectronic materials.[7,8] It is noted that some

* To whom correspondence should be addressed. E-mail: jplang@suda.edu.cn.
† Suzhou University.
‡ Shanghai Institute of Organic Chemistry.

(1) (a) Müller, A.; Diemann, E.; Jostes, R.; Bögge, H. *Angew. Chem., Int. Ed.* **1981**, *20*, 934. (b) Müller, A.; Bögge, H.; Schimanski, U.; Penk, M.; Nieradzik, K.; Dartmann, M.; Krickemeyer, E.; Schimanski, J.; Römer, C.; Römer, M.; Dornfeld, H.; Wienböker, U.; Hellmann, W. *Monatsh. Chem.* **1989**, *120*, 367.

10.1021/ic8019342 CCC: $40.75
Published on Web 02/24/2009

of these clusters, especially those incomplete cubanelike ones, have Cu(I) atoms coordinated by terminal halides or pseudohalides, which can be replaced by various donor ligands to form cluster-supported species. For example, one family of incomplete cubanelike clusters, $[Et_4N]_2[MO(\mu_3\text{-}S)_3(CuX)_3]$ (M = Mo, W; X = CN, NCS, Br),[9,10] were used to react with phosphine ligands and N-donor ligands to yield discrete and polymeric clusters with these ligands coordinated at the Cu(I) site.[11,12] The second family is that of the Cp* analogues $[PPh_4][Cp^*M(\mu_3\text{-}S)_3(CuX)_3]$ (M = Mo, W; X = CN, NCS, Br).[13] They were also employed to react with various P- or N-donor ligands, forming many $[Cp^*M(\mu_3\text{-}S)_3Cu_3]$-based clusters, especially those with intriguing 1D, 2D, and 3D topological structures.[14] The third family is that of the Tp* analogues $[Et_4N][Tp^*W(\mu_3\text{-}S)_3(CuX)_3]$ (Tp* = hydridotris(3,5-dimethylpyrazol-1-yl)borate; X = Cl, Br, I, NCS, CN). However, their reactivity toward different donor ligands seems less explored.

Chart 1. Structures of py, ani, 4,4′-bipy, bpee, bpe, and bpp Ligands

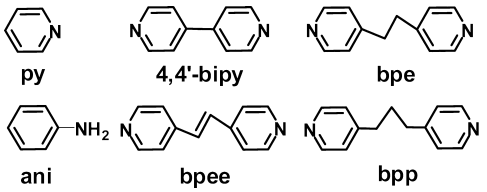

As an extension of our project on the chemistry of Mo(W)/Cu/S clusters, we have recently been engaged in the preparation of W/Cu/S clusters derived from $[Et_4N][Tp^*WS_3]$.[15] It was found that, relative to its Cp* analogue $[PPh_4][Cp^*MS_3]$ (M = Mo, W), $[Et_4N][Tp^*WS_3]$ showed similar reactivity toward CuCl, forming the incomplete cubanelike cluster $[Et_4N][Tp^*W(\mu_3\text{-}S)_3(CuCl)_3]$. However, it also had somewhat different reactivity toward CuNCS or CuCN, forming a rare decanuclear cluster, $[Tp^*W(\mu_3\text{-}S)_3Cu_3(\mu\text{-}NCS)_3(CuMeCN)]_2$, and a polymeric cluster, $[Tp^*W(\mu_3\text{-}S)(\mu\text{-}S)_2Cu_2(MeCN)(\mu\text{-}CN)]_n$.[16] Compared with the reactivity of $[PPh_4][Cp^*M(\mu_3\text{-}S)_3(CuX)_3]$ toward N-donor ligands,[14a,c] do the Tp* analogues show similar performance? What other cluster-based frameworks can be generated? With these questions in mind, we deliberately prepared $[Et_4N][Tp^*W(\mu_3\text{-}S)_3(CuBr)_3]$ (**1**) and chose six N-donor ligands (Chart 1): two monodentate ligands [pyridine (py) and aniline (ani)], two rigid bidentate ligands [4,4′-bipyridine (4,4′-bipy) and 1,2-bis(4-pyridyl)ethylene (bpee)], and two flexible ligands [1,2-bis(4-pyridyl)ethane (bpe) and 1,3-bis(4-pyridyl)propane

(2) (a) Christou, G.; Garner, C. D.; Mabbs, F. E.; King, T. J. *J. Chem. Soc., Chem. Commun.* **1978**, 740. (b) Jeannin, Y.; Sécheresse, F.; Bernes, S.; Robert, F. *Inorg. Chim. Acta* **1992**, *198*−*200*, 493. (c) Coucouvanis, D. *Adv. Inorg. Chem.* **1998**, *104*, 682. (d) Howard, K. E.; Rauchfuss, T. B.; Rheingold, A. L. *J. Am. Chem. Soc.* **1986**, *108*, 297. (e) Holm, R. H. *Pure Appl. Chem.* **1995**, *67*, 217. (f) Shibahara, T. *Coord. Chem. Rev.* **1993**, *123*, 73. (g) Ansari, M. A.; Ibers, J. A. *Coord. Chem. Rev.* **1990**, *100*, 223. (h) Stiefel, E. I.; Coucouvanis, D.; Newton, W. E. Molybdenum Enzymes, Cofactors and Model Systems. *ACS Symposium Series 535*; American Chemical Society: Washington, DC, 1993.

(3) (a) Wu, X. T. *Inorganic Assembly Chemistry*; Science Press and Science Press USA Inc: Beijing, 2004; pp 1−179. (b) Wu, D. X.; Hong, M. C.; Cao, R.; Liu, H. Q. *Inorg. Chem.* **1996**, *35*, 1080.

(4) (a) Ansari, M. A.; Ibers, J. A. *Coord. Chem. Rev.* **1990**, *100*, 223. (b) Hou, H. W.; Xin, X. Q.; Shi, S. *Coord. Chem. Rev.* **1996**, *153*, 25. (c) Coucouvanis, D. *Adv. Inorg. Chem.* **1998**, *45*, 1.

(5) (a) Lang, J. P.; Xin, X. Q. *J. Solid State Chem.* **1994**, *108*, 118. (b) Lang, J. P.; Tatsumi, K. *Inorg. Chem.* **1998**, *37*, 6308. (c) Yu, H.; Xu, Q. F.; Sun, Z. R.; Ji, S. J.; Chen, J. X.; Liu, Q.; Lang, J. P.; Tatsumi, K. *Chem. Commun.* **2001**, 2614. (d) Lang, J. P.; Xu, Q. F.; Yuan, R. X.; Abrahams, B. F. *Angew. Chem., Int. Ed.* **2004**, *43*, 4741. (e) Lang, J. P.; Jiao, C. M.; Qiao, S. B.; Zhang, W. H.; Abrahams, B. F. *Inorg. Chem.* **2005**, *44*, 2664.

(6) (a) Mills, C. F. *Philos. Trans. R. Soc. London, Ser. B* **1979**, *288*, 51. (b) Eldredge, P. A.; Averill, B. A. *J. Cluster Sci.* **1990**, *1*, 269. (c) Stiefel, E. I.; MatsumotoK. Transition Metal Sulfur Chemistry, Biological and Industrial Significance. *ACS Symposium Series 653*; American Chemical Society: Washington, DC, 1996. (d) George, G. N.; Pickering, I. J.; Yu, E. Y.; Prince, R. C.; Bursakov, S. A.; Gavel, O. Y.; Moura, I.; Moura, J. J. G. *J. Am. Chem. Soc.* **2000**, *122*, 8321. (e) Dobbek, H.; Gremer, L.; Kiefersauer, R.; Huber, R.; Meyer, O. *Proc. Natl. Acad. Sci. U. S. A.* **2002**, *99*, 15971. (f) Ginda, M.; Ferner, R.; Gremer, L.; Meyer, O.; Meyer-Klaucke, W. *Biochemistry* **2003**, *42*, 222. (g) George, G. N.; Pickering, I. J.; Harris, H. H.; Gailer, J.; Klein, D.; Lichtmannegger, J. *J. Am. Chem. Soc.* **2003**, *125*, 1704.

(7) (a) Chan, C. K.; Guo, C. X.; Wang, R. J.; Mak, T. C. W.; Che, C. M. *J. Chem. Soc., Dalton Trans.* **1995**, 753. (b) Che, C. M.; Xia, B. H.; Huang, J. S.; Chan, C. K.; Zhou, Z. Y.; Cheung, K. K. *Chem.*−*Eur. J.* **2001**, *7*, 3998.

(8) (a) Shi, S.; Ji, W.; Tang, S. H.; Lang, J. P.; Xin, X. Q. *J. Am. Chem. Soc.* **1994**, *116*, 3615. (b) Shi, S.; Ji, W.; Lang, J. P.; Xin, X. Q. *J. Phys. Chem.* **1994**, *98*, 3570. (c) Zheng, H. G.; Ji, W.; Low, M. L. K.; Sakane, G.; Shibahara, T.; Xin, X. Q. *J. Chem. Soc., Dalton Trans.* **1997**, 2375. (d) Shi, S. In *Optoelectronic Properties of Inorganic Compounds*; Roundhill, D. M., Fackler, J. P., Jr., Eds.; Plenum Press: New York, 1998; pp 55−105. (e) Zhang, C.; Song, Y. L.; Xu, Y.; Fun, H. K.; Fang, G. Y.; Wang, Y. X.; Xin, X. Q. *J. Chem. Soc., Dalton Trans.* **2000**, 2823. (f) Coe, B. J. In *Comprehensive Coordination Chemistry II*; McCleverty, J. A., Meyer, T. J., Eds.; Elsevier Pergamon: Oxford, U. K., 2004; Vol. 9, pp 621−687. (g) Zhang, W. H.; Song, Y. L.; Zhang, Y.; Lang, J. P. *Cryst. Growth Des.* **2008**, *8*, 253.

(9) (a) Hou, H. W.; Xin, X. Q.; Shi, S. *Coord. Chem. Rev.* **1996**, *153*, 25. (b) Lang, J. P.; Ji, S. J.; Xu, Q. F.; Shen, Q.; Tatsumi, K. *Coord. Chem. Rev.* **2003**, *241*, 47.

(10) (a) Müller, A.; Bögge, H.; Schimanski, U. *Inorg. Chim. Acta* **1983**, *69*, 5. (b) Jeannin, Y.; Sécheresse, F.; Bernes, S.; Robert, F. *Inorg. Chim. Acta* **1992**, *198*, 493. (c) Hou, H. W.; Long, D. L.; Xin, X. Q.; Huang, X. Y.; Kang, B. S.; Ge, P.; Ji, W.; Shi, S. *Inorg. Chem.* **1996**, *35*, 5363.

(11) (a) Zheng, H. G.; Jin, Q. H.; Long, D. L.; Xin, X. Q. *Chin. J. Struct. Chem.* **2000**, *19*, 53. (b) Hou, H. W.; Zheng, H. G.; Ang, H. G.; Fan, Y. T.; Low, M. K. M.; Zhu, Y.; Wang, W. L.; Xin, X. Q.; Ji, W.; Wong, W. T. *J. Chem. Soc.; Dalton Trans.* **1999**, 2953. (c) Sécheresse, F.; Robert, F.; Marzak, S.; Manoli, J. M.; Potvin, C. *Inorg. Chim. Acta* **1991**, *182*, 221. (d) Du, S. W.; Zhu, N. Y.; Chen, P. C.; Wu, X. T. *Angew. Chem., Int. Ed.* **1992**, *31*, 1085. (e) Guo, J.; Wu, X. T.; Zhang, W. J.; Sheng, T. L.; Huang, Q.; Lin, P.; Wang, Q. M.; Lu, J. X. *Angew. Chem., Int. Ed.* **1997**, *36*, 2464. (f) Guo, J.; Sheng, T. L.; Zhang, W. J.; Wu, X. T.; Lin, P.; Wang, Q. M.; Lu, J. X. *Inorg. Chem.* **1998**, *37*, 3689.

(12) (a) Huang, Q.; Wu, X. T.; Wang, Q. M.; Sheng, T. L.; Lu, J. X. *Inorg. Chem.* **1996**, *35*, 893. (b) Song, L.; Li, J. R.; Li, P.; Li, Z. H.; Li, T.; Du, S. W.; Wu, X. T. *Inorg. Chem.* **2006**, *45*, 10155. (c) Liang, K.; Zheng, H. G.; Song, Y. L.; Li, Y. Z.; Xin, X. Q. *Cryst. Growth Des.* **2007**, *7*, 373. (d) Li, J. R.; Du, S. W.; Wu, X. T. *J. Cluster Sci.* **2005**, *16*, 489. (e) Zhang, C.; Song, Y. L.; Kuhn, F. E.; Wang, Y. X.; Xin, X. Q.; Herrmann, W. A. *Adv. Mater.* **2002**, *14*, 818. (f) Beheshti, A.; Clegg, W.; Hyvadi, R.; Hekmat, H. F. *Polyhedron* **2002**, *21*, 1547.

(13) (a) Lang, J. P.; Kawaguchi, H.; Ohnishi, S.; Tatsumi, K. *Inorg. Chim. Acta* **1998**, *283*, 136. (b) Lang, J. P.; Kawaguchi, H.; Ohnishi, S.; Tatsumi, K. *Chem. Commun.* **1997**, 405. (c) Lang, J. P.; Xu, Q. F.; Chen, Z. N.; Abrahams, B. F. *J. Am. Chem. Soc.* **2003**, *125*, 12682.

(14) (a) Xu, Q. F.; Chen, J. X.; Zhang, W. H.; Ren, Z. G.; Li, H. X.; Zhang, Y.; Lang, J. P. *Inorg. Chem.* **2006**, *45*, 4055. (b) Lang, J. P.; Xu, Q. F.; Zhang, W. H.; Li, H. X.; Ren, Z. G.; Chen, J. X.; Zhang, Y. *Inorg. Chem.* **2006**, *45*, 10487. (c) Zhang, W. H.; Song, Y. L.; Ren, Z. G.; Li, H. X.; Li, L. L.; Zhang, Y.; Lang, J. P. *Inorg. Chem.* **2007**, *46*, 6647.

(15) (a) Seino, H.; Arai, Y.; Iwata, N.; Nagao, S.; Mizobe, Y.; Hidai, M. *Inorg. Chem.* **2001**, *40*, 1677. (b) Seino, H.; Iwata, N.; Kawarai, N.; Hidai, M.; Mizobe, Y. *Inorg. Chem.* **2003**, *42*, 7387.

(16) Wang, J.; Sun, Z. R.; Deng, L.; Wei, Z. H.; Zhang, W. H.; Zhang, Y.; Lang, J. P. *Inorg. Chem.* **2007**, *46*, 11381.

Chart 2. Designation of Compounds and Abbreviations[a] for **1**−**7**

$[Et_4N][Tp^*W(\mu_3\text{-}S)_3(CuBr)_3]$ (**1**)

$[Tp^*W(\mu_3\text{-}S)_3Cu_3(py)_3(\mu_3\text{-}Br)](PF_6)$ (**2**)

$[\{Tp^*W(\mu_3\text{-}S)_3(CuBr)_3\}(\mu_6\text{-}Br)\{Tp^*W(\mu_3\text{-}S)_3Cu_3(ani)_3\}]\cdot 4ani\cdot 0.5Et_2O$ (**3**·4ani·0.5Et_2O)

$\{[Tp^*W(\mu_3\text{-}S)_3Cu_3(4,4'\text{-bipy})_3(\mu_3\text{-}Br)](PF_6)\cdot H_2O\}_n$ (**4**)

$[\{Tp^*W(\mu_3\text{-}S)_3Cu_3Br_2\}_2(bpee)]\cdot 0.5CH_2Cl_2$ (**5**·0.5CH_2Cl_2)

$\{[\{Tp^*W(\mu_3\text{-}S)_3Cu_3(\mu_3\text{-}Br)\}_2(bpe)_3](PF_6)_2\cdot MeCN\}_n$ (**6**)

$\{[Tp^*W(\mu_3\text{-}S)_3Cu_3Br(\mu_3\text{-}Br)(bpp)]\cdot DMF\}_n$ (**7**)

[a] Tp* = hydridotris(3,5-dimethylpyrazol-1-yl)borate; py = pyridine; ani = aniline; 4,4′-bipy = 4,4′-bipyridine; bpee = 1,2-bis(4-pyridyl)ethylene; bpe = 1,2-bis(4-pyridyl)ethane; bpp = 1,3-bis(4-pyridyl)propane.

(bpp)]. We carried out the reactions of **1** with these N-donor ligands, and six novel $[Tp^*M(\mu_3\text{-}S)_3Cu_3]$-based clusters, **2**−**7** (Chart 2), were isolated therefrom. The crystal structures of **1**−**7**, determined using single-crystal X-ray analysis, are described, and their electronic properties and solution behavior are discussed on the basis of their IR, UV−vis, ^1H NMR, and electrospray ionization (ESI) mass spectra.

Results and Discussion

Synthetic and Spectral Aspects. When **1** was treated with pyridine, the dark-red solution easily went greenish. Only the starting material **1** and some uncharacterized green crystalline solids were isolated from the solution. However, mixing **1** and NH_4PF_6 (molar ratio = 1:3) in excess pyridine followed by a standard workup gave rise to the cationic cluster **2** in 45% yield (Scheme 1). The idea for introducing the large anion salt NH_4PF_6 into this reaction came from the formation of dicationic cluster $[Cp^*W(\mu_3\text{-}S)_3Cu_3(py)_6](PF_6)_2$ from reactions of $[\{Cp^*W(\mu_3\text{-}S)_3\}_3Cu_7(MeCN)_9](PF_6)_4$ with excess pyridine.[17] The different outcomes for the above two reactions may be ascribed to the fact that the Tp* group is more bulky than the Cp* group and thus blocks the second py ligand coordinated at each Cu(I) site of **2**.

Aniline is known to work as a good solvent for dissolving Mo(W)/Cu/S clusters and sometimes as a ligand coordinated to Cu(I).[14c] An analogous treatment of **1** with excess aniline in the presence of NH_4PF_6 followed by a similar workup to that used in the isolation of **2** afforded the neutral octanuclear cluster **3**·4ani·0.5Et_2O in 35% yield (Scheme 1).

On the other hand, the incomplete cubanelike Mo(W)/Cu/S cluster precursors were proved to be reactive toward rigid (e.g., 4,4′-bipy, bpee) and flexible (e.g., bpe, bpp) multidentate N-donor ligands, forming a series of cluster-based supramolecular compounds.[14] For example, $[PPh_4][Cp^*W(\mu_3\text{-}S)_3(CuBr)_3]$ reacted with 4 equiv of 4,4′-bipy to form a 2D polymeric cluster $\{[Cp^*W(\mu_3\text{-}S)_3Cu_3Br(\mu\text{-}Br)(4,4'\text{-bipy})]\cdot Et_2O\}_n$.[14a] The addition of NH_4PF_6 into the solution containing **1** and 4,4′-bipy immediately generated a white precipitate (NH_4Br). Layering of Et_2O onto the filtrate produced the different 2D cationic polymeric cluster **4** (55% yield). Analogous reactions of **1** with bpee and NH_4PF_6 led to the formation of the neutral dimeric cluster **5**·0.5CH_2Cl_2 (60% yield).

Reactions of **1** with bpe in the presence of NH_4PF_6 produced the cationic 1D polymeric cluster **6** (50% yield). Parallel reactions using different cluster-to-ligand molar ratios and different solvent systems such as DMF and aniline did not form any other cluster-based polydimensional complexes with different $[Tp^*W(\mu_3\text{-}S)_3Cu_3]$/bpe ratios but always afforded **6** in ca. 20% yield. Intriguingly, when its Cp* analogue $[PPh_4][Cp^*Mo(\mu_3\text{-}S)_3(CuBr)_3]$ reacted with bpe in DMF or DMSO, or aniline, a set of $[Cp^*Mo(\mu_3\text{-}S)_3Cu_3]$-based polymeric compounds of 1D single- and double-stranded chain structures could be isolated.[18] In the case of bpp, similar reactions afforded another 1D polymeric cluster **7** (65% yield), which is similar to its Cp* analogue $[Cp^*Mo(\mu_3\text{-}S)_3Cu_3(\mu\text{-bpp})(\mu\text{-}Br)Br]_n$ derived from reactions of $[PPh_4][Cp^*Mo(\mu_3\text{-}S)_3(CuBr)_3]$ with bpp in DMF/MeCN.[18]

In order to gain more insight into the behaviors of **1**−**7** in solution, their ESI mass spectra were examined. The assignments were made through the inspection of peak positions and isotopic distributions. The negative ESI mass spectrum of **1** in DMF showed the parent anion ($[Tp^*WS_3Cu_3Br_3]^-$) signal at m/z = 1008.5, which matches well with its theoretical isotopic distributions (Figure S1, Supporting Information). This indicated that the $[Tp^*WS_3Cu_3Br_3]^-$ anion of **1** did exist and was stable in solution. However, the positive ESI-MS of **2** in DMF/MeOH did not exhibit the parent cation peak, but a dicationic peak at m/z = 518.9 for a $[\{Tp^*WS_3Cu_3(py)_3\}+MeOH]^{2+}$ species, which may be originated from the loss of a Br atom from the parent cation of **2** (Figure S2, Supporting Information). The formation of such a species is consistent with the fact that a μ_3-Br atom weakly binds to the three Cu centers in the parent cation, as described later in this paper. For **3**, the positive and negative ESI-MS showed a $[Tp^*WS_3Cu_3Br(ani)_3]^+$ fragment peak at m/z = 1128.6 and a $[Tp^*WS_3Cu_3Br_3]^-$ fragment peak at m/z = 1008.5, respectively, implying that **3** was dissociated in solution (Figure S3, Supporting Information). In fact, these two fragments in the crystal structure of **3** are weakly associated by a μ_6-Br atom. For **4**, the positive ESI mass spectrum presented a peak at m/z = 2701.8 that may be assigned to $[(Tp^*WS_3Cu_3)_2Br_3(4,4'\text{-bipy})_5+2DMF]^+$ species (Figure S4, Supporting Information). The positive ESI-MS of **5** in DMF/EtOH had a peak at m/z = 2084.6 for the parent cationic $[\{Tp^*WS_3Cu_3Br_2\}_2(bpee)+EtOH+H]^+$ species (Figure S5, Supporting Information). For **6**, its positive ESI-MS showed a $[(Tp^*WS_3Cu_3Br)_2(bpe)_3]^{2+}$ dicationic species at m/z = 1124.6 (Figure S6, Supporting Information). Finally, the addition of an equimolar amount of CF_3COOH to the solution of **7** in DMF exhibited two peaks at m/z = 865.5 and 1045.4 assignable to $[Tp^*WS_3Cu_3Br(H_2O)]^+$ and $[Tp^*WS_3Cu_3Br(bpp)]^+$ species (Figure S7, Supporting Information). Both species may be derived from the repeating $[Tp^*W(\mu_3\text{-}S)_3Cu_3Br(\mu_3\text{-}Br)(bpp)]$ unit via a loss of one bromide and

(17) Yu, H.; Zhang, W. H.; Ren, Z. G.; Chen, J. X.; Wang, C. L.; Lang, J. P.; Elim, H. I.; Ji, W. *J. Organomet. Chem.* **2005**, *690*, 4027.

(18) Zhang, W. H.; Song, Y. L.; Wei, Z. H.; Li, L. L.; Huang, Y. J.; Zhang, Y.; Lang, J. P. *Inorg. Chem.* **2008**, *47*, 5332.

Scheme 1. Reactions of **1** with Various N-Donor Ligands in the Presence of NH_4PF_6

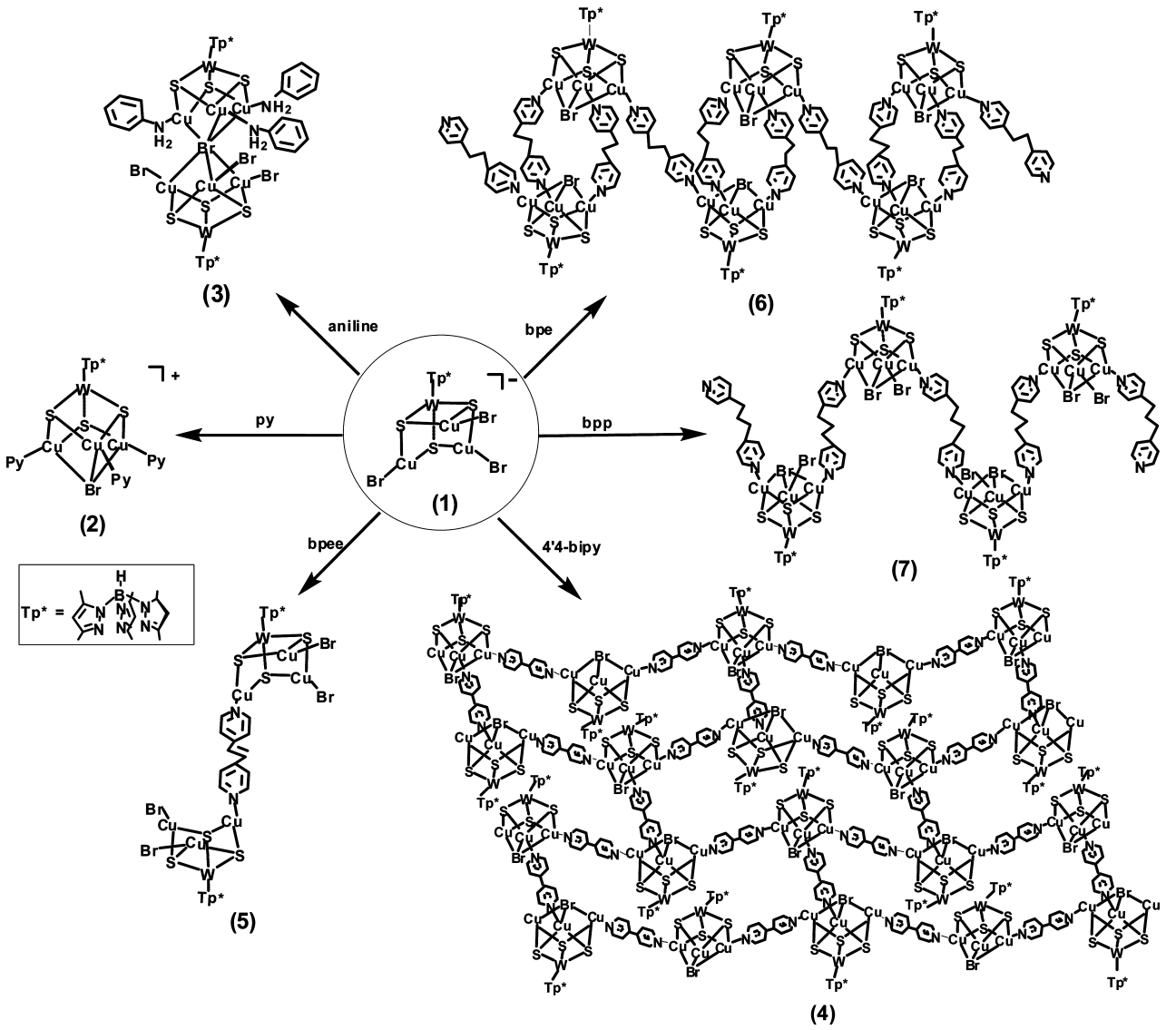

one bpp ligand. From these results, we concluded that the core structure of the monomeric clusters **1** and **2** and the strongly bridged dimeric cluster **5** were retained in DMF, though some peripheral ligands like halides or bridging ligands may be lost under the mass conditions. For the polymeric clusters like **4**, **6**, and **7**, their multidimensional frameworks were no longer maintained in solution and tended to be dissociated into small cluster fragments under the mass

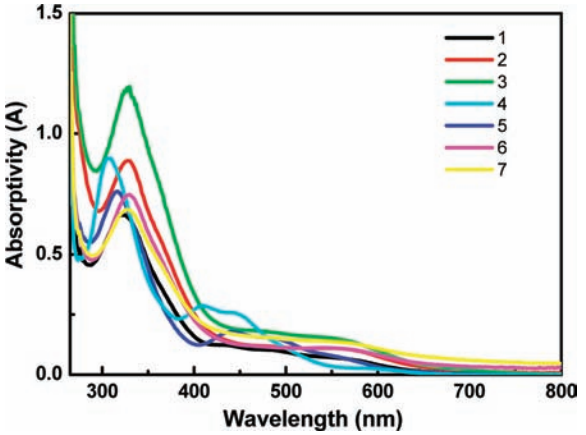

Figure 1. Electronic spectra of **1** (6.8×10^{-5} M), **2** (4.9×10^{-5} M), **3** (3.6×10^{-5} M), **4** (2.7×10^{-5} M), **5** (1.9×10^{-5} M), **6** (5.6×10^{-5} M), and **7** (7.0×10^{-5} M) in DMF in a 1-cm-thick glass cell.

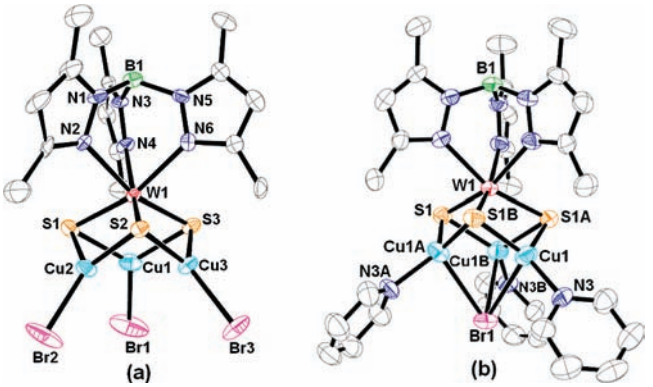

Figure 2. (a) View of the cluster anion of **1**. (b) View of the cluster cation of **2**. The thermal ellipsoids are drawn at 50% probability level. All hydrogen atoms are omitted for clarity. Symmetry codes: A, $-y + 1, x - y + 1, z$; B, $-x + y, -x + 1, z$.

conditions. The identities of **1**−**7** were further confirmed by X-ray crystallography.

Crystal Structures of [Et$_4$N][Tp*W(μ_3-S)$_3$(CuBr)$_3$] (1) and [Tp*W(μ_3-S)$_3$Cu$_3$(py)$_3$(μ_3-Br)](PF$_6$) (2). Compound **1** crystallizes in the monoclinic space group $P2_1/n$, and the asymmetric unit contains one discrete [Tp*W(μ_3-S)$_3$(CuBr)$_3$]$^-$ anion and one [Et$_4$N]$^+$ cation. However, **2** crystallizes in the hexagonal space group $P\bar{3}c1$, and the asymmetric unit contains one-third of the [Tp*W(μ_3-S)$_3$Cu$_3$(py)$_3$(μ_3-Br)]$^+$ cations and two-thirds of the PF_6^- anions. Like its chloride analogue,[15] the structure of the anion in **1** consists of one [Tp*WS$_3$]$^-$ unit and three CuBr units that are held together via μ_3-S atoms to form an incomplete cubanelike [W(μ_3-S)$_3$Cu$_3$] core structure (Figure 2a). The [Tp*W(μ_3-S)$_3$Cu$_3$(py)$_3$(μ_3-Br)]$^+$ cation in **2** contains a distorted cubanelike structure in which one bromide fills into the void of the incomplete cubanelike [Tp*W(μ_3-S)$_3$Cu$_3$] core with three long Cu−μ_3-Br distances (Figure 2b). There is a 3-fold axis going through H1, B1, W1, and Br1. The resulting [W(μ_3-S)$_3$Cu$_3$(μ_3-Br)] cube closely resembles those observed in [Cp*W(μ_3-S)$_3$Cu$_3$(μ_3-Br)(PPh$_3$)$_3$](PF$_6$)[17] and [WS(μ_3-S)$_3$Cu$_3$(μ_3-Br)(PPh$_3$)$_3$]·H$_2$O.[19] As shown in Table 1, the mean W1···Cu contact (2.6390(13) Å) in **1** is almost identical to that of its chloride analogue (2.6404(18) Å), but slightly shorter than those found in the three-coordinated Cu clusters such as **2** (2.6679(13) Å) and [PPh$_4$][Cp*W(μ_3-S)$_3$(CuBr)$_3$] (2.661(1) Å).[13b] The average terminal Cu−Br length (2.272(3) Å) in **1** is slightly shorter than that of [PPh$_4$][Cp*W(μ_3-S)$_3$(CuBr)$_3$] (2.308(1) Å), while the mean Cu−μ_3-Br length (2.7633(18) Å) of **2** is close to that of [WS(μ_3-S)$_3$Cu$_3$(μ_3-Br)(PPh$_3$)$_3$]·H$_2$O (2.761(1) Å),[19] but longer than that of [Cp*W(μ_3-S)$_3$Cu$_3$(μ_3-Br)(PPh$_3$)$_3$](PF$_6$) (2.713(1) Å).[17]

Crystal Structure of [{Tp*W(μ_3-S)$_3$(CuBr)$_3$}(μ_6-Br){Tp*W(μ_3-S)$_3$Cu$_3$(ani)$_3$}]·4ani·0.5Et$_2$O (3·4ani·0.5Et$_2$O). Compound **3**·4ani·0.5Et$_2$O crystallizes in the triclinic space group $P\bar{1}$, and the asymmetric unit contains one discrete [{Tp*W(μ_3-S)$_3$(CuBr)$_3$}(μ_6-Br){Tp*W(μ_3-S)$_3$Cu$_3$(ani)$_3$}] molecule, two aniline and four halves of aniline solvent molecules, and half a diethyl ether solvent molecule. Compound **3** consists of one [Tp*W(μ_3-S)$_3$Cu$_3$(ani)$_3$]$^{2+}$ dication and one [Tp*W(μ_3-S)$_3$Cu$_3$Br$_3$]$^-$ anion, which are bridged by a μ_6-Br atom, forming a corner-shared double cubanelike [{W(μ_3-S)$_3$Cu$_3$}(μ_6-Br){W(μ_3-S)$_3$Cu$_3$}] core structure (Figure 3). This core is closely related to those of the P-cluster structures in the nitrogenases and their mimicked clusters,[20] though in the structures of the latter ones, two incomplete cubanelike [Fe$_4$(μ_3-S)$_3$] cores are linked by a μ_6-S atom. In **3**, the six-coordinate geometry around Br4 can be best described as trigonal antiprism. To our knowledge, the occurrence of such a double cubanelike cluster core with a μ_6-Br atom is unprecedented in the chemistry of [MS$_4$]$^{2-}$ and [Cp*MS$_3$]$^-$ (M = Mo, W). In this core structure, each copper(I) center is coordinated by two μ_3-S atoms and one N atom of the

Table 1. Selected Bond Distances (Å) for Compounds **1**−**7**

		compound **1**	
W(1)···Cu(1)	2.6386(13)	W(1)···Cu(2)	2.6386(13)
W(1)···Cu(3)	2.6399(14)	W(1)−S(1)	2.310(3)
W(1)−S(2)	2.304(2)	W(1)−S(3)	2.312(2)
Cu(1)−S(1)	2.220(3)	Cu(1)−S(3)	2.203(3)
Cu(2)−S(1)	2.207(3)	Cu(2)−S(2)	2.217(3)
Cu(3)−S(2)	2.206(3)	Cu(3)−S(3)	2.224(3)
Cu(1)−Br(1)	2.273(3)	Cu(2)−Br(2)	2.2679(17)
Cu(3)−Br(3)	2.2771(17)		
		compound **2**	
W(1)···Cu(1)	2.6679(13)	W(1)−S(1)	2.302(2)
Cu(1)−S(1A)	2.230(3)	Cu(1)−S(1B)	2.246(3)
Cu(1)−Br(1)	2.7633(18)	Cu(1)−N(3)	1.960(7)
		compound **3**	
W(1)···Cu(1)	2.6451(18)	W(1)···Cu(2)	2.6829(17)
W(1)···Cu(3)	2.696(2)	W(2)···Cu(4)	2.6546(18)
W(2)···Cu(5)	2.6566(16)	W(2)···Cu(6)	2.6740(19)
W(1)−S(1)	2.303(3)	W(1)−S(2)	2.304(3)
W(1)−S(3)	2.302(3)	W(2)−S(4)	2.312(3)
W(2)−S(5)	2.328(3)	W(2)−S(6)	2.304(3)
Cu(1)−S(1)	2.225(4)	Cu(1)−S(2)	2.225(4)
Cu(2)−S(1)	2.217(4)	Cu(2)−S(3)	2.246(4)
Cu(3)−S(2)	2.237(4)	Cu(3)−S(3)	2.240(4)
Cu(4)−S(4)	2.213(3)	Cu(4)−S(5)	2.236(4)
Cu(5)−S(4)	2.223(4)	Cu(5)−S(6)	2.223(4)
Cu(6)−S(5)	2.227(4)	Cu(6)−S(6)	2.220(4)
Cu(1)−Br(1)	2.320(2)	Cu(2)−Br(2)	2.346(2)
Cu(3)−Br(3)	2.372(2)	Cu(1)−Br(4)	3.138(2)
Cu(2)−Br(4)	2.920(2)	Cu(3)−Br(4)	2.798(2)
Cu(4)−Br(4)	2.899(2)	Cu(5)−Br(4)	2.918(2)
Cu(6)−Br(4)	2.797(2)	Cu(4)−N(13)	1.987(11)
Cu(5)−N(14)	2.000(10)	Cu(6)−N(15)	2.010(10)
		compound **4**	
W(1)···Cu(1)	2.646(2)	W(1)···Cu(2)	2.6889(17)
W(1)−S(1)	2.287(4)	W(1)−S(2)	2.298(3)
Cu(1)−S(2)	2.223(4)	Cu(2)−S(2)	2.251(3)
Cu(2)−S(1)	2.238(4)	Cu(1)−N(5)	1.937(14)
Cu(1)−Br(1)	2.734(3)	Cu(2)−Br(1)	2.768(3)
Cu(2)−N(6)	1.989(11)		
		compound **5**	
W(1)···Cu(1)	2.639(2)	W(1)···Cu(2)	2.6525(17)
W(1)···Cu(3)	2.6238(18)	W(1)−S(1)	2.314(3)
W(1)−S(2)	2.311(3)	W(1)−S(3)	2.307(4)
Cu(1)−S(2)	2.216(4)	Cu(1)−S(3)	2.212(4)
Cu(2)−S(1)	2.205(4)	Cu(2)−S(2)	2.215(4)
Cu(3)−S(1)	2.201(4)	Cu(3)−S(3)	2.203(4)
Cu(1)−Br(1)	2.259(2)	Cu(2)−Br(2)	2.277(2)
Cu(3)−N(7)	1.929(11)		
		compound **6**	
W(1)···Cu(1)	2.655(2)	W(1)···Cu(2)	2.6594(17)
W(1)···Cu(3)	2.6881(15)	W(1)−S(1)	2.313(3)
W(1)−S(2)	2.285(3)	W(1)−S(3)	2.295(3)
Cu(1)−S(1)	2.242(3)	Cu(1)−S(2)	2.221(3)
Cu(2)−S(1)	2.241(3)	Cu(2)−S(3)	2.228(3)
Cu(3)−S(2)	2.248(3)	Cu(3)−S(3)	2.268(3)
Cu(1)−N(7)	1.961(9)	Cu(2)−N(8)	1.971(9)
Cu(3)−N(9)	1.970(10)	Cu(1)−Br(1)	2.834(2)
Cu(2)−Br(1)	2.664(2)	Cu(3)−Br(1)	2.720(3)
		compound **7**	
W(1)···Cu(1)	2.6873(19)	W(1)···Cu(2)	2.655(2)
W(1)···Cu(3)	2.7166(19)	W(1)−S(1)	2.296(4)
W(1)−S(2)	2.296(4)	W(1)−S(3)	2.306(4)
Cu(1)−S(1)	2.252(4)	Cu(1)−S(2)	2.246(4)
Cu(2)−S(2)	2.239(4)	Cu(2)−S(3)	2.232(4)
Cu(3)−S(1)	2.256(4)	Cu(3)−S(3)	2.241(4)
Cu(1)−Br(1)	2.631(3)	Cu(2)−Br(1)	2.794(2)
Cu(3)−Br(1)	2.727(3)	Cu(3)−Br(2)	2.341(2)
Cu(2)−N(8)	1.956(13)		

(19) Lang, J. P.; Zhu, H. Z.; Xin, X. Q.; Chen, M. Q.; Liu, K.; Zheng, P. J. *Chin. J. Chem.* **1993**, *11*, 21.
(20) (a) Zhang, Y. G.; Zuo, J. L.; Zhou, H. C.; Holm, R. H. *J. Am. Chem. Soc.* **2002**, *124*, 14292. (b) Zuo, J. L.; Zhou, H. C.; Holm, R. H. *Inorg. Chem.* **2003**, *42*, 4624. (c) Zhang, Y. G.; Holm, R. H. *J. Am. Chem. Soc.* **2003**, *125*, 3910. (d) Zhang, Y. G.; Holm, R. H. *Inorg. Chem.* **2004**, *43*, 674. (e) Berlinguette, C. P.; Miyaji, T.; Zhang, Y. G.; Holm, R. H. *Inorg. Chem.* **2006**, *45*, 1997. (f) Berlinguette, C. P.; Holm, R. H. *J. Am. Chem. Soc.* **2006**, *128*, 11993.

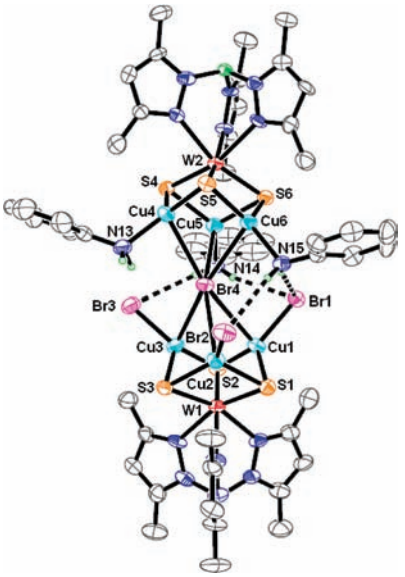

Figure 3. Molecular structure of **3** with 50% thermal ellipsoid. All of the hydrogen atoms except those of the coordinated aniline molecules are omitted for clarity.

coordinated aniline molecule (Cu1, Cu2, Cu3) or one terminal Br atom (Cu4, Cu5, Cu6), forming an approximate trigonal planar coordination with a fourth weak Cu−μ_6-Br interaction (Table 1). The six W···Cu contacts are in the range of 2.6451(18)−2.696(2) Å, and their mean value (2.6682(17) Å) is almost the same as that of **2**. The six Cu−μ_6-Br distances vary from 2.797(2) to 3.138(2) Å, which are much longer than those of the Cu−μ_3-Br distances of **2**. It should be noted that, within the molecule, the three terminal Br atoms interact with the H atoms of the two coordinated aniline molecules to afford four strong intramolecular H bonds (N14−H14A···Br1 2.669 Å, N14−H14B···Br3 2.760 Å, N15−H15A···Br1 2.735 Å, and N15−H15B···Br2 2.716 Å). These hydrogen-bonding interactions may play some role in the stabilization of this cluster molecule.

Crystal Structures of {[Tp*W(μ_3-S)$_3$Cu$_3$(4,4′-bipy)$_3$(μ_3-Br)](PF$_6$)·H$_2$O}$_n$ (4) and [{Tp*W(μ_3-S)$_3$Cu$_3$Br$_2$}$_2$(bpee)]·0.5CH$_2$Cl$_2$ (5·0.5CH$_2$Cl$_2$). Compound **4** crystallizes in the monoclinic space group *C2/m*, and the asymmetric unit contains half of a [Tp*W(μ_3-S)$_3$Cu$_3$(4,4′-bipy)$_3$(μ_3-Br)] cation, one PF_6^- anion, and two halves of water solvent molecules. Whereas, **5**·0.5CH_2Cl_2 crystallizes in the triclinic space group $P\bar{1}$, and the asymmetric unit contains half of a [{Tp*W(μ_3-S)$_3$Cu$_3$Br$_2$}$_2$(bpee)] molecule and half of a CH_2Cl_2 solvent molecule. The [Tp*W(μ_3-S)$_3$Cu$_3$(4,4′-bipy)$_3$(μ_3-Br)] cation in **4** adopts a similar core structure to that of **2** and has a mirror plane running through the W1, Cu1, Br1, B1, S1, N1, N2, N5, C1−C5, and C16−C18 atoms (Figure 4a). From a topological perspective, such a cation may be visualized as being a pyramidal three-connecting node. The occurrence of such a node is rare in the cluster-supported supramolecular chemistry. Six of such nodes interconnect through six 4,4′-bipy bridges, forming a chairlike cyclohexane-shaped [{Tp*W(μ_3-S)$_3$Cu$_3$(μ_3-Br)}$_6$(4,4′-bipy)$_9$] unit (the red parallelogram part in Figure 4b). The neighboring cyclohexane-like units are further fused into a 2D (6,3) network that extends along the *bc* plane. The average layer-to-layer separation is ca. 11.55 Å with the PF_6^- anions and water solvent molecules locating between the [Tp*W(μ_3-S)$_3$Cu$_3$(4,4′-bipy)$_3$(μ_3-Br)]$_n^{n-}$ cationic layers.

On the other hand, the [(Tp*W(μ_3-S)$_3$Cu$_3$Br$_2$)$_2$(bpee)] molecule in **5** is composed of two incomplete cubanelike [Tp*W(μ_3-S)$_3$Cu$_3$Br$_2$] fragments linked by a bridging bpee ligand, forming a new type of double incomplete cubanelike structure (Figure 5). There is a crystallographic center of symmetry located on the middle point of the C21−C21A bond. Interestingly, this discrete molecule is ca. 2.9 nm long in one direction (from C1 to C1A) and thus may be viewed as a nanoscale cluster, which is uncommon in the chemistry of thiometallates.

Each Cu atom in **4** adopts an approximate trigonal planar coordination with a fourth weak Cu−μ_3-Br bond (Table 1). The average W1···Cu separation and W−μ_3-S, Cu−μ_3-S, Cu−N, and Cu−μ_3-Br bond lengths of **4** are all similar to those of the corresponding ones of **2**. The mean W···Cu, W−μ_3-S, and Cu−μ_3-S bond lengths in **5** are normal relative to those of the corresponding ones in **1**. The mean Cu−N(py) length at 1.929(11) Å is shorter than those of **2** (1.960(7) Å) and **4** (1.966(14) Å).

Crystal Structures of {[{Tp*W(μ_3-S)$_3$Cu$_3$(μ_3-Br)}$_2$(bpe)$_3$](PF$_6$)$_2$·MeCN}$_n$ (6) and {[Tp*W(μ_3-S)$_3$Cu$_3$Br(μ_3-Br)(bpp)]·DMF}$_n$ (7). Compound **6** crystallizes in triclinic space group $P\bar{1}$, and the asymmetric unit contains two halves of [{Tp*W(μ_3-S)$_3$Cu$_3$(μ_3-Br)}$_2$(bpe)$_3$]$^{2+}$ dications, two PF_6^- anions, and one MeCN solvent molecule. Whereas, **7** crystallizes in the monoclinic space group $P2_1/c$, and the asymmetric unit contains one [Tp*W(μ_3-S)$_3$Cu$_3$Br(μ_3-Br)(bpp)] molecule and one DMF solvent molecule. As the two cluster dications in **6** are chemically identical, only the perspective view of one of them is shown in Figure 6a. Each [{Tp*W(μ_3-S)$_3$Cu$_3$(μ_3-Br)}$_2$(bpe)$_3$]$^{2+}$ dication in **6** shows a dimeric squarelike structure, in which two [Tp*W(μ_3-S)$_3$Cu$_3$(μ_3-Br)] fragments are connected with a pair of bpe bridges. There is a crystallographic inversion center lying at the midpoint of the W1 and W1A contact. The structure of each cubanelike [Tp*W(μ_3-S)$_3$Cu$_3$(μ_3-Br)] fragment in **6** closely resembles those of **2** and **4**. Topologically, each [Tp*W(μ_3-S)$_3$Cu$_3$(μ_3-Br)] fragment works as an angular two-connecting node that interconnects its neighboring ones alternatively via double bpe bridges and single bpe bridges, forming a 1D zigzag chain extending along the *b* axis (Figure 6b). Alternatively, this zigzag chain can be viewed as being built up of the dimeric [{Tp*W(μ_3-S)$_3$Cu$_3$(μ_3-Br)}$_2$(bpe)$_2$] units that are linked via single bpe bridges.

The structure of the cubanelike [Tp*W(μ_3-S)$_3$Cu$_3$Br(μ_3-Br)(bpp)] molecule in **7** (Figure 7a) is close to those of **2**, **4**, and **6**. Each copper(I) center is coordinated by two μ_3-S atoms and one N atom of the bpp ligand (Cu1, Cu2) or one terminal Br atom (Cu3), forming an approximate trigonal planar coordination with a fourth weak Cu−μ_3-Br interaction. From a topological perspective view, the [Tp*W(μ_3-S)$_3$Cu$_3$Br(μ_3-Br)] core in **7** acts as a two-connecting node, which links two equivalent cores via two bpp ligands to form a one-dimensional spiral chain extending along the *b* axis (Figure 7b). Because **7** crystallizes in the symmetric space

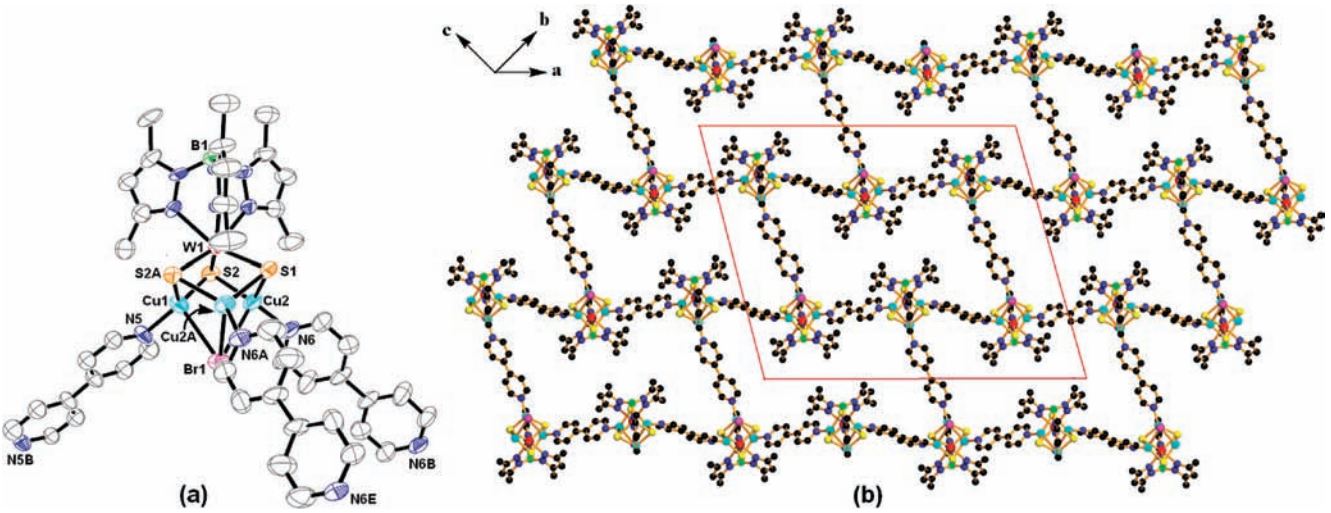

Figure 4. (a) View of the [Tp*W(μ_3-S)$_3$Cu$_3$(4,4-bipy)$_3$(μ_3-Br)] structure of **4** with 50% thermal ellipsoids. (b) Extended 2D structure of **4** looking down the *c* axis. The chairlike cyclohexane-shaped repeating unit was highlighted by the red parallelogram. All hydrogen atoms were omitted for clarity. Symmetry codes: A, x, $-y-1$, z; B, $-x$, $-y-1$, $-z+2$; E, $0.5-x$, $-0.5-y$, $-z+1$.

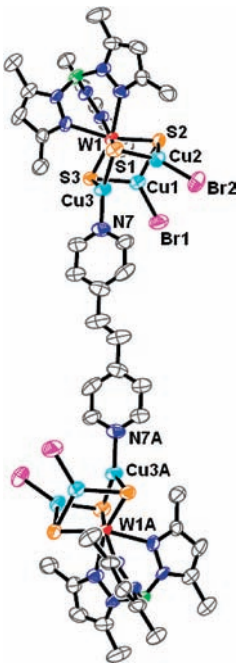

Figure 5. Molecular structure of **5** with 50% thermal ellipsoids. All hydrogen atoms are omitted for clarity. Symmetry code: A, $-x-1$, $-y$, $-z-1$.

group, there are two helical strands with opposite chirality in a unit cell. The average chain-to-chain separation is ca. 5.3 Å. Between chains are situated the bulky Tp* groups. Each 1D chain stacks along the *b* axis to generate a 1D channel with a rhombic opening. The channels occupy a total volume of 672.6 Å^3 (16.7% of the total cell volume calculated by the *Platon* program) and are filled with DMF solvent molecules (Figure 7c). The μ_3-Br atoms of the cluster interact with the H atoms of the methyl groups of the DMF molecules to afford intermolecular H-bonding interactions (C30−H30D···Br1 2.930 Å). Besides, the O atoms of the DMF molecules also interact with the H atom of methylene groups of the bpp ligand to form the other intermolecular H-bonding interactions (C22−H22B···O1 2.678 Å). These two kinds of intermolecular hydrogen-bonding interactions keep the DMF molecules sitting in the 1D channel.

In **6**, the W1···Cu1 and W1···Cu2 contacts are relatively shorter than that of W1···Cu3 (Table 1). Their average value (2.664(2) Å) is close to those of **2** and **4**, but somewhat shorter than that of **7** (2.686(19) Å). The average Cu−μ_3-S, W−μ_3-S, Cu−N bond lengths in **6** and **7** are normal. Within the [{Tp*W(μ_3-S)$_3$Cu$_3$(μ_3-Br)}$_2$(bpe)$_2$] unit of **6**, the two bpe ligands show a trans−trans conformation, while those linking such units present a trans−gauche conformation. Each bpp ligand in **7** adopts only a trans−trans conformation.

Conclusions

In this paper, we explored the construction of a family of monomeric, dimeric, and polymeric W/Cu/S clusters (**2**−**7**) from reactions of a preformed cluster [Et$_4$N][Tp*W-(μ_3-S)$_3$(CuBr)$_3$] (**1**) with monodentate, rigid, and flexible bidentate N-donor ligands under the presence of NH_4PF_6. The results demonstrated that reactions of **1** with monodentate ligands like py and aniline may form discrete clusters, while those of **1** with rigid bidentate ligands (e.g., 4,4′-bipy) prefer forming more symmetric structures and those of **1** with flexible ones (e.g., bpe and bpp) tend to yield low-dimensional structures. In all of these compounds, the cluster [Tp*W(μ_3-S)$_3$Cu$_3$] core structure of **1** was retained. The topological frameworks of some of these clusters like **3** and **4** are unprecedented in the chemistry of tetrathiometallates and Cp*-coordinated trithiometallates. Isolation of **2**−**7** suggested that **1** is an excellent precursor for the W/Cu/S cluster-based assemblies. According to the results of the ESI mass spectra of **1**−**7**, the core structures of the monomeric or dimeric clusters like **1**, **2**, and **5** survived in solution, while the polymeric clusters like **3**, **4**, **6** and **7** did not keep their solid-state structures in solution and were broken into small cluster fragments under the mass conditions. It is believed that these small cluster fragments observed at mass conditions may be instructive and helpful for our rational design and construction of new W/Cu/S cluster-based suppramolecular arrays using **1** and other analogues as precursors. We are

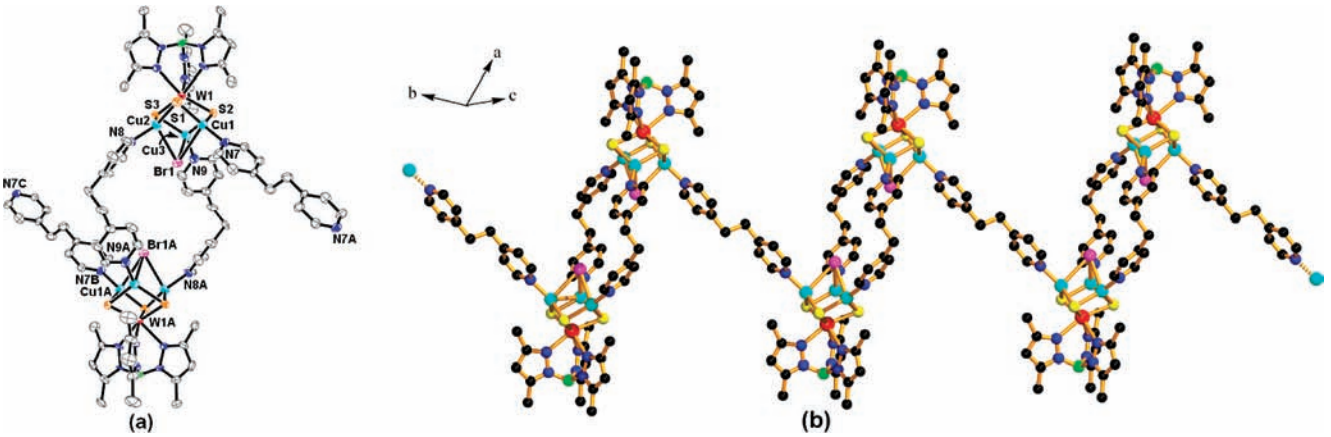

Figure 6. (a) View of the $[\{Tp^*W(\mu_3\text{-}S)_3Cu_3(\mu_3\text{-}Br)\}_2(bpe)_4]$ dimeric structure of **6** with 50% thermal ellipsoids. (b) View of a section of the 1D zigzag chain (extended along the *b* direction) in **6**. All hydrogen atoms were omitted for clarity. Symmetry codes: A, $-x$, $-y + 2$, $-z$; B, $-x$, $-y + 1$, $-z$; C, x, $y - 1$, z.

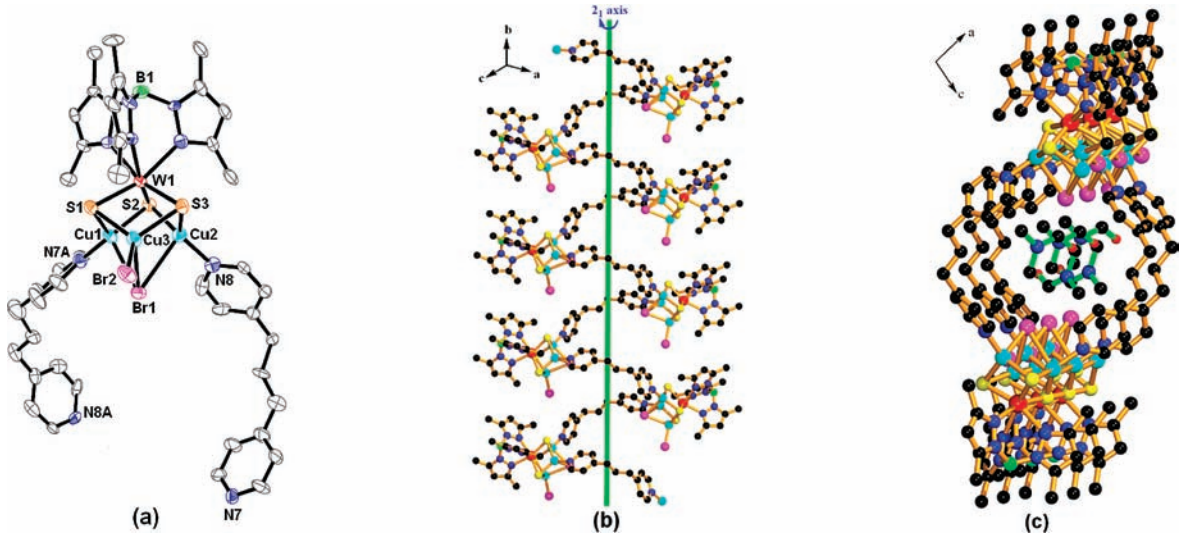

Figure 7. (a) Perspective view of the $[Tp^*W(\mu_3\text{-}S)_3Cu_3Br(\mu_3\text{-}Br)(bpp)_2]$ molecule of **7** with 50% thermal ellipsoids. (b) View of a section of the 1D spiral chain of **7** extending along the *b* axis. (c) Side view of the chain structure of **7** along the *b* axis. All hydrogen atoms are omitted for clarity. Symmetry code: A, $-x + 1$, $0.5 + y$, $0.5 - z$.

currently extending this work in studies on the assembly of novel cluster-based arrays from reactions of **1** with other multidentate N-donor ligands such as 2,4,6-tri(4-pyridyl)-1,3,5-triazine and 1,3,5-tris(3,5-dimethyl-pyrazolyl-1-ylmethyl)-2,4,6-trimethylbenzene.[21]

Experimental Section

General Procedures. All manipulations were performed under an argon atmosphere using standard Schlenk-line techniques. $[Et_4N][Tp^*WS_3]\cdot MeCN$ was prepared as reported previously.[15] Aniline and DMF were freshly distilled under reduced pressure, while other solvents were predried over activated molecular sieves and refluxed over the appropriate drying agents under argon. ^1H NMR spectra were measured at ambient temperatures on a Varian UNITYplus-400 spectrometer. ^1H NMR chemical shifts were referenced to TMS in $CDCl_3$ or in deuterated dimethyl sulfoxide (DMSO-d_6) signal. IR spectra were recorded on a Varian 1000 FT-IR spectrometer as KBr disks (4000−400 cm^{-1}). UV−vis spectra were measured on a Varian 50 UV−visible spectrophotometer. Elemental analyses for C, H, and N were performed on a Carlo-Erba CHNO-S microanalyzer. ESI mass spectra were performed on a DECAX-30000 LCQ Deca XP mass spectrometer.

$[Et_4N][Tp^*W(\mu_3\text{-}S)_3(CuBr)_3]$ (1). To a solution of $[Et_4N][Tp^*WS_3]\cdot MeCN$ (75 mg, 0.1 mmol) in 15 mL of $CHCl_3$ was added CuBr (43 mg, 0.3 mmol). The mixture was stirred for half an hour and filtered. Diethyl ether (4 mL) was carefully layered onto the surface of the purple red filtrate (2 mL) in a glass tube (length = 25 cm, $\varphi = 0.6$ cm), which was then capped with a rubber septum. The glass tube was allowed to stand at room temperature for 2 days, forming dark red prisms of **1**, which were collected by filtration, washed thoroughly with Et_2O, and dried in vacuo. Yield: 106 mg (90% based on **1**). Anal. calcd for $C_{23}H_{41}N_7BBr_3WCu_3S_3$: C, 24.30; H, 3.63; N, 8.62. Found: C, 24.32; H, 3.55; N, 8.95. IR (KBr disk): 2978 (m), 2920 (m), 2554 (w), 1628 (w), 1546 (s), 1440 (s), 1435 (s), 1418 (s), 1035 (m), 860 (w), 806 (w), 691 (w), 651 (w), 479 (w), 410 (w) cm^{-1}. UV−vis (DMF, λ_{max} (nm (ε M^{-1} cm^{-1}))): 323 (10 300), 440 (8400), 554 (6000). ^1H NMR (400 MHz,

(21) Hartshorn, C. M.; Steel, P. J. *Aust. J. Chem.* **1995**, *48*, 1587.

Table 3. Crystallographic Data for **1**, **2**, **3**·4ani·0.5Et_2O, **4**, **5**·0.5CH_2Cl_2, **6**, and **7**

compounds	**1**	**2**	**3**·4ani·0.5Et_2O
chemical formula	$C_{23}H_{41}BBr_3Cu_3N_7S_3W$	$C_{30}H_{37}BBrCu_3F_6N_9PS_3W$	$C_{74}H_{98}B_2Br_4Cu_6N_{19}O_{0.5}S_6W_2$
fw	1136.84	1230.07	2544.34
cryst syst	monoclinic	hexagonal	triclinic
space group	$P2_1/n$	$P\bar{3}c1$	$P\bar{1}$
a (Å)	10.090(2)	13.7343(19)	13.125(3)
b (Å)	36.391(7)	13.7343(19)	14.905(3)
c (Å)	10.091(2)	24.610(5)	28.681(6)
α (deg)	78.16		
β (deg)	95.85	79.76(3)	
γ (deg)	120	70.15(3)	
V (Å^3)	3686.0(13)	4020.3(11)	5129.6(18)
Z	4	4	1
D_{calcd} (g·cm^{-3})	2.049	2.032	1.648
F(000)	2188	2330	2494
μ (Mo Kα, cm^{-1})	8.267	5.664	5.178
total no. of reflns.	27233	33380	49737
no. of unique reflns.	6609 (R_{int} = 0.0911)	2466 (R_{int} = 0.0685)	18594 (R_{int} = 0.0691)
no. of variables	365	175	903
R^a	0.0598	0.0651	0.0806
wR^b	0.1314	0.1032	0.1855
GOF^c	1.091	1.323	1.112
residual peaks (e/Å^3)	1.562	1.578	1.975

compounds	**4**	**5**·0.5CH_2Cl_2	**6**	**7**
chemical formula	$C_{60}H_{68}B_2Br_2Cu_6F_{12}N_{18}O_2P_2S_6W_2$	$C_{42.5}H_{55}B_2Br_4ClCu_6N_{14}S_6W_2$	$C_{68}H_{81}B_2Br_2Cu_6F_{12}N_{19}P_2S_6W_2$	$C_{31}H_{43}BBr_2Cu_3N_9OS_3W$
fw	2488.03	2080.08	2577.28	1199.06
cryst syst	monoclinic	triclinic	triclinic	monoclinic
space group	$C2/m$	$P\bar{1}$	$P\bar{1}$	$P2_1/c$
a (Å)	28.987(6)	11.347(2)	16.328(3)	16.996(3)
b (Å)	16.351(3)	11.437(2)	17.671(4)	10.512(2)
c (Å)	11.547(2)	16.618(3)	18.614(4)	22.559(5)
α (deg)		107.82(3)	108.40(3)	
β (deg)	100.29(3)	97.93(3)	100.25(3)	90.39(3)
γ (deg)		110.02(3)	112.32(3)	
V (Å^3)	5384.9(19)	1856.6(6)	4434.7(15)	4030.3(14)
Z	2	1	2	4
D_{calcd} (g·cm^{-3})	1.532	1.860	1.93	1.974
F(000)	2408	993	2512	2332
μ (Mo Kα, cm^{-1})	4.237	7.162	5.147	6.583
total no. of reflns.	26599	18313	39265	38505
no. of unique reflns.	5103 (R_{int} = 0.0793)	6760 (R_{int} = 0.0532)	15760 (R_{int} = 0.0645)	7365 (R_{int} = 0.1225)
no. of variables	303	359	1083	464
R^a	0.0825	0.0681	0.0713	0.0952
wR^b	0.2109	0.1543	0.1474	0.1836
GOF^c	1.082	1.005	1.136	1.187
residual peaks (e/Å^3)	1.647	1.323	2.283	1.818

^{a} $R_1 = \sum||F_o| - |F_c||/\sum|F_o|$. ^{b} $wR_2 = \{w\sum(|F_o| - |F_c|)^2/\sum w|F_o|^2\}\}^{1/2}$. ^{c} GOF = $\{\sum w(|F_o| - |F_c|)^2/(n-p)\}^{1/2}$, where n is the number of reflections and p is total number of parameters refined.

$CDCl_3$): δ 1.36−1.40 (t, 12H, CH_2CH_3), 2.37 (s, 9H, CH_3 in Tp*), 2.95 (s, 9H, CH_3 in Tp*), 3.33−3.39 (q, 8H, CH_2CH_3), 5.94 (s, 3H, C*H* in Tp*). The B−H proton was not located.

[Tp*W(μ_3-S)$_3$Cu$_3$Py$_3$(μ_3-Br)](PF$_6$) (2). Compound **1** (57 mg, 0.05 mmol) was dissolved in 5 mL of pyridine in the presence of NH_4PF_6 (25 mg, 0.15 mmol). A workup similar to that used for the isolation of **1** formed deep red blocks of **2** two weeks later, which were collected by filtration, washed thoroughly with Et_2O, and dried in vacuo. Yield: 28 mg (45%). Anal. calcd for $C_{30}H_{37}BBrCu_3F_6N_9PS_3W$: C, 29.29; H, 3.03; N, 10.25. Found: C, 29.78; H, 2.85; N, 10.96. IR (KBr disk): 2965 (m), 2923 (m), 2555 (m), 1634 (S), 1547 (S), 1415 (s), 1350 (s), 1095 (m), 1026 (m), 846 (s), 558 (m), 459 (m) cm^{-1}. UV−vis (DMF, λ_{max} (nm (ε M^{-1} cm^{-1}))): 327 (24 600), 477 (20 390), 550 (5800). ^{1}H NMR (400 MHz, $CDCl_3$): δ 2.37 (s, 9H, CH_3 in Tp*), 2.80 (s, 9H, CH_3 in Tp*), 6.09 (s, 3H, C*H* in Tp*), 7.38−8.54 (m, 15*H*, py). The B−H proton was not located.

[{Tp*W(μ_3-S)$_3$(CuBr)$_3$}(μ_6-Br){Tp*W(μ_3-S)$_3$Cu$_3$(ani)$_3$}]·4ani·0.5Et$_2$O (3·4ani·0.5Et$_2$O). To a solution of **1** (57 mg, 0.05 mmol) in 5 mL of aniline was added NH_4PF_6 (25 mg, 0.15 mmol). A workup similar to that used for the isolation of **1** afforded deep-red blocks of **3**·4ani·0.5Et_2O three weeks later, which were collected by filtration, washed thoroughly with 1:4 v/v MeCN/Et_2O, and dried in vacuo. Yield: 18 mg (35%). Anal. calcd for $C_{148}H_{196}B_4Br_8Cu_{12}N_{38}OS_{12}W_4$: C, 34.93; H, 3.88; N, 10.46. Found: C, 35.78; H, 3.45; N, 10.32. IR (KBr disk): 2973 (m), 2912 (m), 2558 (m), 1610 (s), 1481 (s), 1377 (s), 1095 (s), 1026 (s), 528 (m), 439 (m) cm^{-1}. UV−vis (DMF, λ_{max} (nm (ε M^{-1} cm^{-1}))): 327 (23 500), 560 (13 800). ^{1}H NMR (400 MHz, DMSO-d_6): δ 1.12 (t, 3H, CH_3 in Et_2O), 2.36 (s, 18H, CH_3 in Tp*), 2.81 (s, 18H, CH_3 in Tp*), 3.42 (q, 2H, CH_2 in Et_2O), 4.99 (s, 14H, PhNH_2), 6.08 (s, 6H, C*H* in Tp*), 6.47−6.99 (m, 35H, phenyl group in aniline). The B−H proton was not located.

{[Tp*WS$_3$Cu$_3$(4,4′-bipy)$_3$(μ_3-Br)](PF$_6$)·H$_2$O}$_n$ (4). To 10 mL of MeCN solution containing **1** (57 mg, 0.05 mmol) was added 4,4′-bipy (31 mg, 0.2 mmol) and NH_4PF_6 (33 mg, 0.2 mmol). A great quantity of white precipitate was formed immediately. The red slurry was stirred for 10 min and filtered. A workup similar to that used for the isolation of **1** afforded red blocks of **4**, which were collected by filtration, washed with Et_2O, and dried in vacuo.

Yield: 68 mg (55%). Anal. calcd for $C_{60}H_{70}B_2Br_2Cu_6F_{12}N_{18}P_2O_2S_6W_2$: C, 28.96; H, 2.84; N, 10.13. Found: C, 28.36; H, 2.60; N, 10.76. IR (KBr disk): 2973 (w), 2912 (w), 2565(m), 1614 (m), 1546 (s), 1436 (s), 1222 (s), 1073 (m), 1036 (m), 844 (s), 692 (vs), 651 (vs), 558 (m), 445 (w), 426 (w) cm^{-1}. UV−vis (DMF, λ_{max} (nm (ε M^{-1} cm^{-1}))): 307 (33 500), 408 (19 800), 447 (15 500). ^{1}H NMR (400 MHz, DMSO-d$_6$): δ 2.37 (s, 9H, CH$_3$ in Tp*), 2.79 (s, 9H, CH$_3$ in Tp*), 6.10 (s, 3H, CH in Tp*), 7.59−8.40 (m, 16H, py in 4,4′-bipy). The B−H proton was not located.

[(Tp*W(μ_3-S)$_3$Cu$_3$Br$_2$)$_2$(bpee)]·0.5CH$_2$Cl$_2$ (5·0.5CH$_2$Cl$_2$). To a 10 mL MeCN solution containing **1** (57 mg, 0.05 mmol) and NH_4PF_6 (33 mg, 0.2 mmol) was added bpee (36 mg, 0.2 mmol) in 5 mL of CH_2Cl_2. A workup similar to that used for the isolation of **4** produced red blocks of **5**·0.5CH_2Cl_2, which were collected by filtration, washed with Et_2O, and dried in vacuo. Yield: 62 mg (60%). Anal. calcd for $C_{42.5}H_{55}B_2Br_4ClCu_6N_{14}S_6W_2$: C, 24.54; H, 2.67; N, 9.43. Found: C, 24.36; H, 3.11; N, 9.36. IR (KBr disk): 2969 (m), 2920 (m), 2563 (m), 1605 (w), 1548 (S) 1483 (s), 1436 (s), 1376 (m), 1108 (s), 996 (m), 753 (m), 726 (s), 690 (s), 537 (s), 465 (w), 423 (w) cm^{-1}. UV−vis (DMF, λ_{max} (nm (ε M^{-1} cm^{-1}))): 315 (38 600), 438 (13 600), 489 (6850). ^{1}H NMR (400 MHz, $CDCl_3$): δ 2.37 (s, 18H, C*H*$_3$ in Tp*), 2.95 (s, 18H, C*H*$_3$ in Tp*), 5.94 (s, 6H, C*H* in Tp*), 7.05 (br s, 2H, −CH═CH−), 8.01−8.91 (m, 8H, py in bpee). The B−H proton was not located.

{[{Tp*W(μ_3-S)$_3$Cu$_3$(μ_3-Br)}$_2$(bpe)$_3$](PF$_6$)$_2$·MeCN}$_n$ (6). To a MeCN solution containing **1** (57 mg, 0.05 mmol) was added bpe (37 mg, 0.2 mmol) and NH_4PF_6 (33 mg, 0.2 mmol). A workup similar to that used for the isolation of **4** generated red blocks of **6**, which were collected by filtration, washed with Et_2O, and dried in vacuo. Yield: 26 mg (50%). Anal. calcd for $C_{68}H_{81}B_2Br_2Cu_6F_{12}N_{19}P_2S_6W_2$: C, 31.69; H, 3.17; N, 10.33. Found: C, 31.57; H, 3.30; N, 9.96. IR (KBr disk): 2979 (m), 2564 (m), 2160 (m), 1483 (m), 1436 (s), 1376 (m), 1108 (vs), 996 (m), 845 (vs), 724 (s), 690 (s), 558 (m), 527 (s), 445 (w), 430 (w) cm^{-1}. UV−vis (DMF, λ_{max} (nm (ε M^{-1} cm^{-1}))): 327 (13 300), 564 (3800). ^{1}H NMR (400 MHz, DMDO-d_6): δ 2.06 (3H, C*H*$_3$ in MeCN), 2.37 (s, 18H, C*H*$_3$ in Tp*), 2.84 (s, 18H, C*H*$_3$ in Tp*), 2.88 (br s, 12H, C*H*$_2$ in bpe), 6.10 (s, 6H, C*H* in Tp*), 7.52−8.70 (m, 24H, py in bpe). The B−H proton was not located.

{[Tp*WS$_3$Cu$_3$Br(μ_3-Br)(bpp)]·DMF}$_n$ (7). To a DMF solution containing **1** (57 mg, 0.05 mmol) was added bpp (40 mg, 0.2 mmol) and NH_4PF_6 (33 mg, 0.2 mmol). A workup similar to that used for the isolation of **1** afforded red blocks of **7**, which were collected by filtration, washed with Et_2O, and dried in vacuo. Yield: 39 mg (65%). Anal. calcd for $C_{31}H_{43}BBr_2Cu_3N_9OS_3W$: C, 31.05; H, 3.61; N, 10.51. Found: C, 31.36; H, 3.06; N, 10.76. IR (KBr disk): 2962 (m), 2924 (m), 2559 (m), 1661 (s), 1615 (s), 1545 (s), 1413 (s), 1350 (s), 1226 (s), 1070 (s), 1034 (s), 796 (m), 691 (w), 652 (w), 521 (w), 415 (w) cm^{-1}. UV−vis (DMF, λ_{max} (nm (ε M^{-1} cm^{-1}))): 327 (10 300), 561 (3400). ^{1}H NMR (400 MHz, DMSO-d_6): δ 1.96 (t, 4H, CH_2CH$_2$CH_2 in bpp), 2.48 (br s, 2H, CH$_2$CH_2CH$_2$ in bpp), 2.52 (s, 9H, C*H*$_3$ in Tp*), 2.73 (s, 3H, C*H*$_3$ in DMF), 2.89 (s, 3H, C*H*$_3$ in DMF), 3.02 (s, 9H, C*H*$_3$ in Tp*), 6.03 (s, 3H, C*H* in Tp*), 7.36−8.50 (m, 8H, py in bpp). The B−H proton and the C−H proton of DMF were not located.

X-Ray Structure Determination. X-ray-quality single crystals of **1**−**7** were obtained directly from the above preparations. All measurements were made on a Rigaku Mercury CCD X-ray diffractometer using graphite monochromated Mo Kα (λ = 0.71070 nm). Each crystal was mounted at the top of a glass fiber and cooled at 193 K in a stream of gaseous nitrogen. Cell parameters were refined by using the program CrystalClear (Rigaku and MSc, version 1.3, 2001) at all observed reflections. The collected data were reduced using the program CrystalClear. The reflection data were also corrected for Lorentz and polarization effects.

The crystal structures of **1**−**7** were solved by direct methods and refined on F^2 using full-matrix least-squares techniques with the SHELXTL-97 program.[22] For **1**, each ethyl group of the Et_4N^+ cation was split into two sites with an occupancy factor of 0.497/0.503 for C16-C23/C16A-C23A. Br(1) was also found to be disordered over two positions with an occupancy ratio of 0.8:0.2 for Br1/Br1A. For **3**·4ani·0.5Et_2O, four aniline solvent molecules and one Et_2O solvent molecule were refined with an occupancy factor of 0.5 due to the weak diffraction of the crystal. In addition, we were unable to model the disorder of the phenyl ring C37−C42, and it was refined as a rigid group. For **4**, the site-occupation factor of the oxygen atoms of two water molecules was also fixed at 0.25. Because of partial evaporation of the solvated CH_2Cl_2 molecules in **5**·0.5CH_2Cl_2, the site-occupation factor for C22, Cl1, and Cl2 atoms was fixed at 0.25. For **1**−**7**, all non-hydrogen atoms, except for those of the disordered Et_4N group in **1**, the aniline solvent molecules, Et_2O molecules, the rigid phenyl ring in **3**·4ani·0.5Et_2O, the water solvent molecules in **4**, and the CH_2Cl_2 solvent molecules in **5**·0.5CH_2Cl_2 were refined anisotropically. Hydrogen atoms for N13, N14, and N15 atoms of the coordinated aniline molecules in **3**·4ani·0.5Et_2O were located from Fourier maps. Hydrogen atoms for the oxygen atoms of the water solvent molecules in **4** were not located. Other hydrogen atoms including the aniline solvent molecules and the B−H were placed in geometrically idealized positions (C−H = 0.98 Å, with U_{iso}(H) =1.5U_{eq}(C) for methyl groups; C−H = 0.99 Å, with U_{iso}(H) =1.2U_{eq}(C) for methylene groups; C−H = 0.95 Å, with U_{iso}(H) =1.2U_{eq}(C) for aromatic rings) and constrained to ride on their parent atoms. A summary of the key crystallographic information for **1**−**7** is tabulated in Table 3.

Acknowledgment. This work was supported by the National Natural Science Foundation of China (Grant nos. 20525101 and 20871088), the State Key Laboratory of Organometallic Chemistry of Shanghai Institute of Organic Chemistry (Grant no. 08-25), the "Qin-Lan" Project of Jiangsu Province, and the "SooChow Scholar" Program and Program for Innovative Research Team of Suzhou University. Prof. Z. N. Chen of FJIRSM is highly appreciated for his kind assistance in measuring ESI mass spectra of **1**−**7**. The authors also give thanks for the helpful suggestions from the editor and the reviewers.

Supporting Information Available: Crystallographic data of **1**−**7** (CIF) and ESI mass spectra of **1**−**7** in PDF format. This material is available free of charge via the Internet at http://pubs.acs.org.

IC8019342

(22) (a) Sheldrick, G. M. *SHELXS-97*; University of Göttingen: Göttingen, Germany, 1997. (b) Sheldrick, G. M. *SHELXL-97*; University of Göttingen: Göttingen, Germany, 1997.